# A Selective, Orally Bioavailable 1,2,4-Triazolo[1,5-a]pyridine-Based Inhibitor of Janus Kinase 2 for Use in Anticancer Therapy: Discovery of CEP-33779

Benjamin J. Dugan,* Diane E. Gingrich, Eugen F. Mesaros, Karen L. Milkiewicz, Matthew A. Curry, Allison L. Zulli, Pawel Dobrzanski, Cynthia Serdikoff, Mahfuza Jan, Thelma S. Angeles, Mark S. Albom, Jennifer L. Mason, Lisa D. Aimone, Sheryl L. Meyer, Zeqi Huang, Kevin J. Wells-Knecht, Mark A. Ator, Bruce A. Ruggeri, and Bruce D. Dorsey

Worldwide Discovery Research, Cephalon, Inc., 145 Brandywine Parkway, West Chester, Pennsylvania 19380, United States

ABSTRACT: Members of the JAK family of nonreceptor tyrosine kinases play a critical role in the growth and progression of many cancers and in inflammatory diseases. JAK2 has emerged as a leading therapeutic target for oncology, providing a rationale for the development of a selective JAK2 inhibitor. A program to optimize selective JAK2 inhibitors to combat cancer while reducing the risk of immune suppression associated with JAK3 inhibition was undertaken. The structure−activity relationships and biological evaluation of a novel series of compounds based on a 1,2,4-triazolo[1,5-a]pyridine scaffold are reported. *Para* substitution on the aryl at the C8 position of the core was optimum for JAK2 potency (**17**). Substitution at the C2 nitrogen position was required for cell potency (**21**). Interestingly, *meta* substitution of C2-NH-aryl moiety provided exceptional selectivity for JAK2 over JAK3 (**23**). These efforts led to the discovery of CEP-33779 (**29**), a novel, selective, and orally bioavailable inhibitor of JAK2.
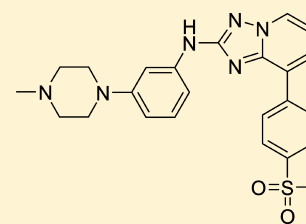
INTRODUCTION

The JAK/STAT signaling pathway is constitutively activated in a wide spectrum of hematopoietic and solid[1] human tumors and high levels of activation are often associated with a more malignant and refractory disease, suggesting an important role in tumor growth and progression. Indeed, there is a growing understanding that the constitutively activated JAK/STAT signaling contributes to tumorigenesis and tumor progression through multiple mechanisms including promoting proliferation and increased antiapoptotic signaling in tumor cells as well as mediating tumor-promoting functions of the stromal compartment. The latter includes tumor-associated inflammation,[2] tumor immune evasion, and angiogenesis. The vast preclinical and clinical evidence supports targeting the JAK/STAT pathway in oncology and inflammatory diseases.[3]

The Janus (JAK) family of nonreceptor tyrosine kinases consists of four members: JAK1, JAK2, JAK3, and TYK2.[4] There is growing evidence demonstrating that JAK2 activation may be particularly critical for tumor growth and progression,[5] supporting its selection as a therapeutic target. In addition, JAK3 inhibition has been shown to be immunosuppressive,[6] providing further rationale for development of a highly selective JAK2 inhibitor. JAK1 and TYK2 have been implicated in disease and immune suppression;[7] however, activity or selectivity against these kinases coupled with inhibition of JAK2 is not adequately understood.

Several JAK inhibitors from a range of chemical classes, including 2-aminopyrimidines, 2,4-diaminopyrimidines, pyrrolopyrimidines, indolocarbazoles, and macrocycles, have been disclosed in the literature with several inhibitors such as

CYT387 (**1**),[8] TG101348 (**2**),[9] INCB018424, ruxolitinib (**3**),[10] AZD1480 (**4**),[11] CEP-701, lestaurtinib (**5**),[12] and SB1518, pacritinib[13] advancing to clinical development (Figure 1).

The 1,2,4-triazolo[1,5-a]pyridine heterocycle[14] provided a novel hinge binding motif for the design of small-molecule ATP-competitive JAK2 inhibitors. The hypothesis was that triazole nitrogen N3 and the exocyclic NH would serve as the H-acceptor and H-donor, respectively, forming hydrogen bonds with the NH and the carbonyl of Leu-932, leading to a strong two-point interaction with the hinge (Figure 2A). On the basis of knowledge from our work with other kinase inhibitor scaffolds,[15] the core would then be modified with various substituents that would drive potency and selectivity while the exocyclic nitrogen would be substituted with various solubilizing groups, as this portion of the molecule would be directed toward the solvent region. This design hypothesis and working model was confirmed later in our program when a JAK2/inhibitor cocrystal structure was solved by X-ray (Figure 2B, vide infra).

CHEMISTRY

A number of literature[16] methods to prepare the 1,2,4-triazolo[1,5-a]pyridine core are known and were evaluated and adapted to meet our design modifications. Initially, we had envisioned target molecules arising from the addition of 2-aminopyridines **6** to arylisothiocyanates **7** to give key intermediates **8**, followed by cyclization to triazolopyridines **9**
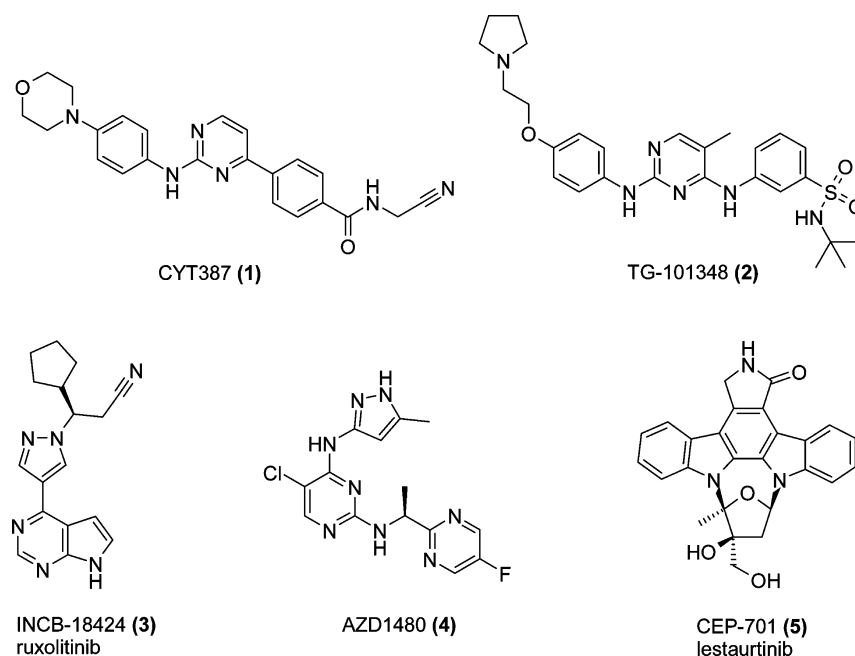
Figure 1. Examples of reported JAK inhibitors.
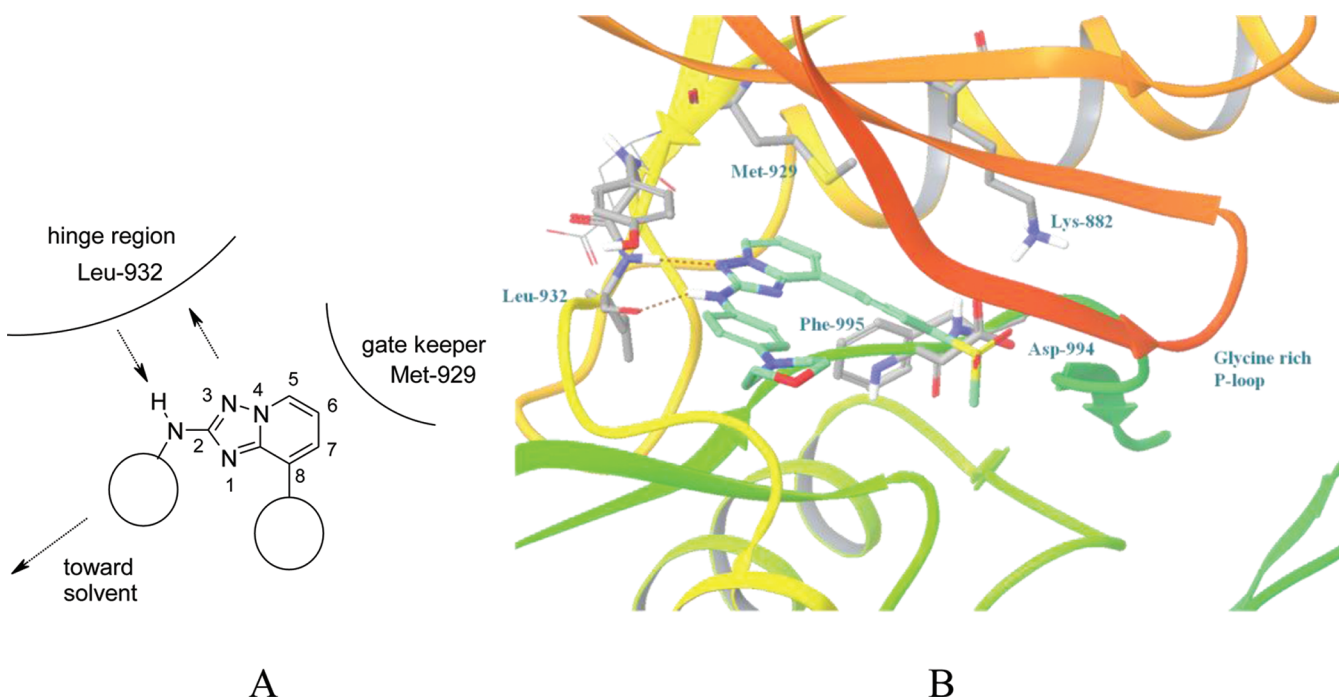

A   B

Figure 2. (A) Design rationale. (B) Ribbon representation of JAK2/inhibitor cocrystal structure with **28**: N-terminal domain in orange, C-terminal domain in green, hinge region in yellow, glycine rich P-loop in darker orange. Key amino acid residues: gatekeeper Met-929, hinge binder Leu-932, and back-pocket salt-bridge of Asp-994 and Lys-882 are explicitly shown in element color-coded stick model. Inhibitor **28** is represented in a stick model: C, green; N, blue; O, red; S, yellow.

(Scheme 1). This methodology was employed for the initial target, 2-phenylamino-1,2,4-triazolo[1,5-*a*]pyridine **9** (X, R = H) via cyclization of the corresponding commercially available thiourea **8** (X, R = H). The core triazolopyridines **9** (where X = Br, R = OCH$_3$) were prepared similarly and were subjected to Suzuki−Miyaura cross coupling with 4-methanesulfonylphenylboronic acid to furnish inhibitors **22−24** (Scheme 1). However, this synthetic route was complicated by poor coupling reactivity for the 2-aminopyridines and arylisothiocyanates and tedious

workups and purifications required at several intermediate steps. The thiourea moiety required activation by *S*-alkylation before addition of hydroxylamine hydrochloride, limiting the use of certain desirable heterocyclic arylisothiocyanates. The cyclization step required the use of phosgene, as ethylchloroformate did not effect this transformation.[17] Ultimately, low overall yields coupled with the scarcity of commercially available arylisothiocyanates or appropriately substituted

Scheme 1. Initial Synthesis of Triazolopyridine Derivatives 9 and 22−24[a]

R = H or OCH$_3$
X = H or Br
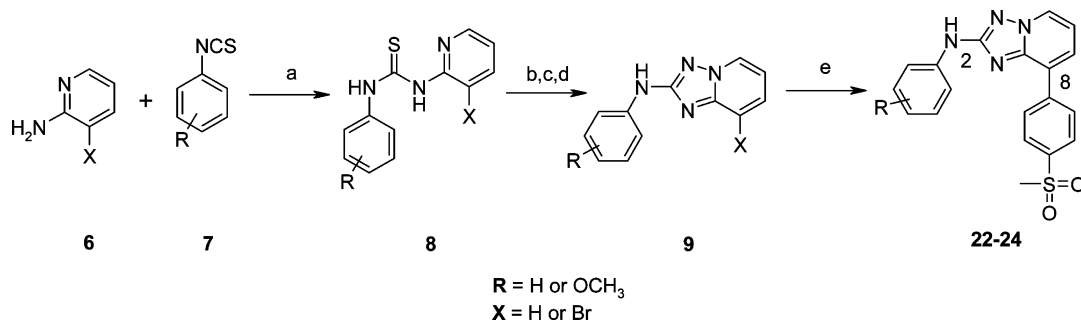
[a]Reagents and conditions: (a) NaH, *p*-dioxane, 0 °C to RT, 66−96%; (b) (CH$_3$O)$_2$SO$_2$, *p*-dioxane, 60 °C; (c) NH$_2$OH hydrochloride, (*i*-Pr)$_2$NEt or K$_2$CO$_3$, *p*-dioxane, 90 °C; (d) 20% phosgene in toluene, K$_2$CO$_3$, acetonitrile, RT, 12−58%; (e) Pd(OAc)$_2$, TPP, 4-methanesulfonylboronic acid, Na$_2$CO$_3$, water, *p*-dioxane, 80 °C, 39−67%. See also Table 3 (**22−24**).

Scheme 2. Improved Synthesis of Triazolopyridine Derivatives 12−21 and 25−41[a]
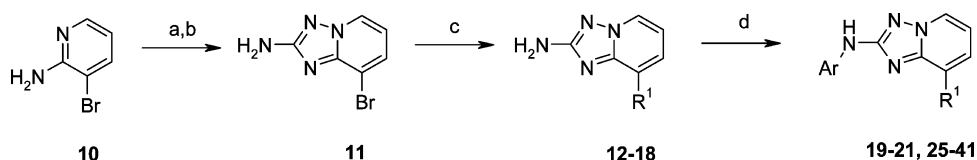
[a]Reagents and conditions: (a) ethoxycarbonyl isothiocyanate, *p*-dioxane, RT; (b) NH$_2$OH hydrochloride, (*i*-Pr)$_2$NEt, EtOH, MeOH, 60 °C, 70%; (c) Pd(OAc)$_2$, TPP, R^1-boronic acid/ester, Na$_2$CO$_3$, water, *p*-dioxane, 80 °C, 8−95%; (d) Pd(OAc)$_2$, ligand, arylbromide, Cs$_2$CO$_3$, *p*-dioxane, 80 °C, 6−77%. See also Table 1 (**12−18**), Table 2 (**19−21**), and Table 3 (**25−41**).

thioureas precluded further SAR optimization by this methodology.

Therefore, a convergent synthesis, suitable for medicinal chemistry purposes, was brought to fruition. Preparation of a core building block substituted with orthogonal synthetic handles (cf. **11** in Scheme 2), in which diversity could be built upon to develop SAR in a timely manner, was accomplished. The core 2-amino-8-bromo-1,2,4-triazolo[1,5-*a*]pyridine[18] **11** was prepared in a "one-pot" process from 2-amino-3-bromopyridine **10**. This synthetic methodology did not require the use of phosgene or ethylchloroformate to effect cyclization. The ethoxycarbonyl isothiocyanate reagent coupled with various aminopyridines to provide activated thioureas that readily reacted with hydroxylamine hydrochloride. Subsequent, in situ, cyclization with concomitant loss of carbon dioxide yielded desired intermediate in good yields.[14] The core was sequentially decorated utilizing a Suzuki−Miyaura cross-coupling reaction with diverse arylboronic acids or esters, followed by subjecting the intermediates **12−18** (Scheme 2) to Buchwald−Hartwig coupling with arylbromides to furnish the desired *N*-arylated products **19−21** and **25−41** in moderate overall yields and in relatively few synthetic steps.

■ RESULTS AND DISCUSSION

The 1,2,4-triazolo[1,5-*a*]pyridine scaffold was quickly shown to exhibit inherent activity against JAK2, as demonstrated by compound **9** (JAK2 IC$_{50}$ = 1089 nM; X, R = H), a molecule that attained moderate potency despite its structural simplicity: a C2 NH-phenyl scaffold. Initial structure−activity relationship studies focused on the C8 position of the triazolopyridine. Substitution in this position greatly influenced JAK2 binding potency, even without an aryl group at the C2 nitrogen (i.e., C2-NH$_2$, see Table 1). An electron rich aryl such as the *ortho* methoxy **12** showed moderate loss of JAK2 activity compared to **9** (X, R = H). Surprisingly, an electron deficient heterocycle
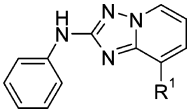
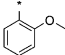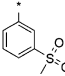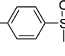**Table 1. Effect of C8 Substitution on C2-NH$_2$ Triazolopyridines**

Ex.	R^1	IC$_{50}$[a,b] (nM)	
		JAK2	JAK3
12		2132	>3000
13		>10,000	>10,000
14		2874	>10,000
15		1406	>10,000
16		2165	>10,000
17		47±20	>2000
18		193±38	>3000

[a]IC$_{50}$ values are reported as the average of at least two separate determinations; for ≥ three determinations, standard deviations are included. [b]see ref 23 for JAK2 assay information.

like the 3-pyridyl **13** was essentially devoid of activity at the highest concentration tested; however, activity was regained upon addition of a methoxy containing pyridyl moiety **14**.

Table 2. Effect of C8 Substitution of C2-NH-Phenyl Derivatives

Ex.	R[1]	IC$_{50}$[a] (nM)		JAK2 Cell	JAK3/2 ratio	Cell/enz ratio
		JAK2	JAK3			
19	(2-methoxyphenyl)	136±53	834±379	-	6	-
20	(3-methanesulfonylphenyl)	8±1	475±70	1071±80	59	134
21	(4-methanesulfonylphenyl)	1.5±0.4	95±43	385±48	63	257

[a]IC$_{50}$ values are reported as the average of at least three separate determinations, standard deviations are included.

Some electron-deficient heterocycles such as the 4-pyridyl (**15**) and substituted aryl moieties containing electron-withdrawing groups (**16−18**) showed promising activity against JAK2 especially when substituted at the *para* position (cf. **17** and **18**). Selectivity for JAK2 over JAK3 was observed for **17** and **18**. However, cellular potency was poor for compounds unsubstituted at the C2 nitrogen (e.g., **17**, IC$_{50}$ >10 μM).

Improving cellular activity was targeted next in order for this scaffold to receive further consideration. On the basis of knowledge developed on other internal programs, it was hypothesized that an increase in lipophilicity would positively impact cellular activity. Efforts to increase the cell membrane permeability focused on appending an aryl group on C2-NH$_2$ molecules to raise lipophilicity.

Table 2 outlines the activity of *N*-phenyl molecules: C2-NHPh substitution was combined with selected C8 substituents (cf. Table 1), which caused a >20-fold boost in JAK2 potency (compare **19−21** to **9**, and **12**, **16**, **17**). Notably, **21** showed excellent JAK2 potency and selectivity. This molecule also exhibited activity, albeit modest, in the cellular assay. The combination of the *para*-substituted aryl at the C8 position and N-arylation at the C2 position displayed the favorable properties of potent JAK2 enzyme inhibition and submicromolar cellular potency and was explored further.
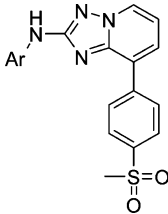
A methoxy scan was undertaken to optimize the C2-NH-aryl moiety (Table 3). While *ortho* substitution was not favored (**22**), either *meta* or *para* substitution showed a positive response, both **23** and **24** having single-digit nanomolar activity against JAK2 with selectivity against JAK3. An increase in cell potency was also observed. Optimization was continued by varying the substituents in the *meta* and *para* positions. Addition of the electron withdrawing methanesulfonyl moiety (**25** and **26**) resulted in potent JAK2 inhibitors with selectivity against JAK3 but at the expense of JAK2 cell potency with **25**. Saturated heterocycles, especially those containing basic functionality, were considered to be good in improving cell permeability and pharmacokinetics. A systematic probe was initiated to evaluate this hypothesis. Addition of a morpholine moiety in compounds **27** and **28** provided subnanomolar inhibitors with selectivity against JAK3 and good cell potency. Importantly, greater selectivity over JAK3 was observed for
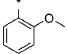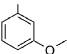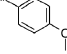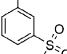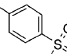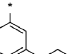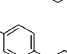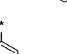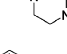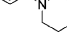
compound **27**. This improved selectivity for JAK2 over JAK3 with a *meta* substituted aryl group was observed throughout the optimization process. The addition of the basic *N*-methyl-piperidine moiety was beneficial: molecules **29** and **30** exhibited good JAK2 enzyme and cell potency. The *meta* derivative **29** was superior to **30** in terms of selectivity versus JAK3 and JAK1 (JAK1 IC$_{50}$ = 81 and 22 nM, respectively), suggesting that further SAR refinement of the *meta* regioisomers should be targeted. Moving the basic functionality away from the aryl group by inserting a methylene− (**31**, **32**) to the saturated heterocycles yielded potent JAK2 inhibitors. Unfortunately, this modification had a deleterious effect on JAK2 cell potency compared to **29**. The basic functionality was extended toward the solvent to give morpholinyl-piperidine **33** and piperidinyl-piperidine **34**. Both compounds were selective against JAK3, and **33** showed good cell activity. C-linked piperidine **35** exhibited excellent cell potency and good selectivity against JAK3 and JAK1 (JAK1 IC$_{50}$ = 43 nM).

Investigations into the role of the *para*-methanesulfonyl group at C8 with bioisosteric electron withdrawing group replacements lead to some interesting results (Table 4). Increasing the size of the alkyl group from methyl to isopropyl (**36**) decreased selectivity against JAK3. Replacement of the sulfone with trifluoromethyl (**37**) led to a potent inhibitor; however, a disappointing loss of cell activity was observed. The fluoro derivative **38** showed a significant loss of potency when compared to the methanesulfonyl derivative **29**. Bioisosteric replacement of methanesulfonyl with dimethylphosphine oxide[19] generated **39**, which exhibited good potency and JAK3 selectivity; however, cellular activity dropped 5-fold.
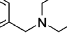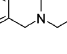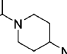
On the basis of their in vitro activity and selectivity profile, compounds **29**, **33**, and **35** were selected for evaluation of off-target liabilities. Compound **33** showed an unfavorable CYP 3A4 inhibition (IC$_{50}$ = 0.2 μM) and was deprioritized. Compounds **29** and **35** did not exhibit CYP 3A4 concerns (IC$_{50}$ = 11 and 24 μM, respectively). Both molecules exhibited acceptable in vitro liver microsome stability in mouse, rat and human (all >15 min) while stability in dog was less than desirable (Table 5). Inhibitors **29** and **35** showed excellent kinase selectivity[20] (S(90) = 0.090 and 0.097, respectively) and were evaluated in vivo (vide infra).

Table 3. Effect of Aryl Substitution in C2-NH-Aryl Derivatives

Ex.	Ar	IC$_{50}$[a] (nM)		JAK2 Cell	JAK3/2 ratio	Cell/enz ratio
		JAK2	JAK3			
22		1615±346	>10,000	-	-	-
23		1.4±0.5	89±33	176±41	63	126
24		3±2	63±24	209±65	21	70
25		5.6±0.6	598±94	490±84	107	88
26		1.3±0.1	105±29	118±21	81	91
27		0.8±0.4	31±5	110±45	39	138
28		0.9±0.1	17±5	61±16	9	68
29		1.8±0.6	150±37	61±12	83	34
30		3±1	31±7	64±18	10	21
31		3.1±0.7	146±12	345±77	47	111
32		0.64±0.07	39±7	107±6	60	167
33		1.1±0.5	60±14	89±10	54	81
34		1.4±0.2	122±49	177±37	87	126
35		0.7±0.1	72±25	50±5	103	71

[a] IC$_{50}$ values are reported as the average of at least three separate determinations, standard deviations are included.

X-Ray Crystallographic Data. A cocrystal structure obtained with **28** in JAK2 catalytic domain (Figure 2B) confirmed the initial hypothesis on the docking of triazopyr- idine into the JAK2 ATP-binding site. Intermolecular hydrogen bonding was observed as designed: triazolopyridine nitrogen N(3) and exocyclic N(2)-H established interactions with the

Table 4. Optimization of the *para* Position
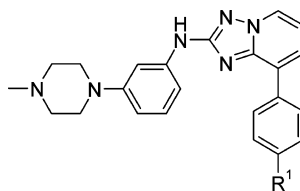
| ex | R¹ | IC₅₀ᵃ (nM) | | | JAK3/2 ratio | cell/enz ratio |
		JAK2	JAK3	JAK2 Cell		
29	SO_2CH_3	1.8 ± 0.6	150 ± 37	61 ± 12	83	34
36	$SO_2\text{-}i\text{-propyl}$	1.27 ± 0.09	38 ± 11	85 ± 10	29	65
37	CF_3	4 ± 1	218 ± 27	476 ± 70	55	119
38	F	26 ± 6	547 ± 119		21	
39	$(P{=}O)(CH_3)_2$	3 ± 1	286 ± 122	318 ± 49	95	106

ᵃIC₅₀ values are reported as the average of at least three separate determinations, standard deviations are included.

Table 5. In Vitro Liver Microsome Stability Expressed as Half-Lives ($t_{1/2}$)

| | $t_{1/2}$ (min) | | | |
ex	mouse	rat	dog	human
29	20	27	5	40
35	40	40	8	40

NH and the carbonyl, respectively, of JAK2 hinge residue Leu-932. The heterocyclic-aromatic aniline fragment at position 2 was exposed to solvent region. The C(8) substituent was located in the binding pocket adjacent to the Lys-882−Asp-994 salt bridge and extended toward the glycine rich P-loop where the methanesulfonyl moiety was involved in water mediated hydrogen bonding interactions. The C(6)-H portion of the core was in the proximity of the gate keeper residue Met-929. Indeed, substitution at the C6 position of the triazolopyridine core in **30** to give derivatives **40** (R(C6) = CF_3) and **41** (R(C6) = F) was accompanied by a severe drop in intrinsic potency for **40** (JAK2 IC₅₀ = >10 μM), likely from a steric clash of the large −CF_3 fragment with Met-929, and only by a moderate loss of potency in case of **41** (JAK2 IC₅₀ = 32 nM), with a significantly smaller fluorine substituent.

Lead Evaluation/Pharmacokinetics/Pharmacodynamics/Efficacy. On the basis of their intrinsic and cellular potency, JAK3/2 selectivity, kinase selectivity, CYP450 inhibition profile, and liver microsome stability, lead molecules **29** and **35** were selected to advance to single dose pharmacokinetic (PK) experiments in mouse. Plasma exposure post oral dosing in CD-1 mouse of each molecule was evaluated. At a single 30 mg/kg, po dose, plasma levels observed for **29** and **35** at 6 h were 535 and 257 ng/mL, respectively. Compound **29** was also tested in nude mouse (Table 6) and exhibited a favorable PK profile, an iv half-life of 1 h, moderate distribution (V_d = 2.6 L/kg), and measurable oral exposure with an estimated bioavailability of 33%. On the basis of the 2-fold higher plasma exposure in CD-1 mouse, the PK

profile in nude mouse, JAK2 enzyme selectivity of 83 and the cellular to enzyme ratio of 34, **29** was selected for in vivo PK/PD evaluation in a single dose study. JAK2 inhibition was monitored by determining levels of STAT3 phosphorylation.

The results from the single dose PK/PD experiments with **29** in CWR22[5a] prostate carcinoma tumor xenografts in nude mouse are shown in Figure 3. The 55 mg/kg oral dose
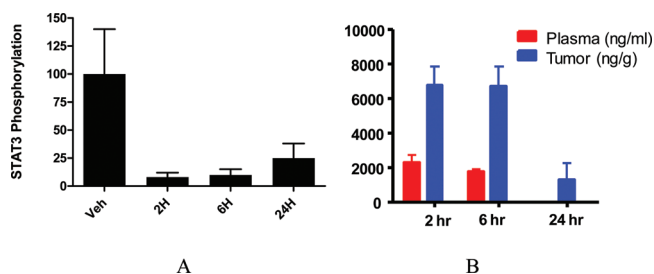
Figure 3. Results of PK/PD experiment in CWR22 xenograft in nude mouse: (A) percent inhibition of STAT3 activation with a single dose of **29** (55 mg/kg po as a solution in PEG400), (B) plasma and tumor compound concentration.

exhibited a pharmacodynamic effect in CWR22 xenografts over 24 h postdose with ≥90% inhibition of STAT3 phosphorylation at the 2 and 6 h time points (Figure 3A). The levels in plasma reached 4−5 μM for up to 6 h, with levels dropping below the minimum quantifiable level (MQL) at 24 h (Figure 3B). Tumor levels were approximately 3-fold higher than plasma levels out to 6 h and were still measurable 24 h postdose. As shown in Figure 4, compound **29** demonstrated antitumor efficacy in the CWR22 xenograft model; oral dosing for 14 days at 30 mg/kg bid resulted in tumor stasis and partial regressions in 5/10 animals. No body weight loss or overt toxicity was noted with this dosing regimen.

In addition to solid tumors, the JAK/STAT pathway is implicated in the tumorigenesis of multiple hematopoietic cancers. Classical Hodgkin lymphoma (cHL) is characterized

Table 6. Single Dose Pharmacokinetic Profiles of 29 in Nude Mouse (Nu/Nu)

species	doseᵃ (mg/kg)	$t_{1/2}$ (h)	AUC₀→∞ (ng·h/mL)	V_d (L/kg)	CL ((mL/min)/kg)	C_{max} (ng/mL)	F (%)
nude	1 iv	1.0	590	2.6	28		
	30 po	1.9	5791			1331	33

ᵃFormulated as solutions in 25% hydroxyl-propyl-β-cyclodextrin (iv) and 100% PEG400 (po).

Figure 4. Antitumor efficacy of **29** in CWR22 xenograft model, dosed po as a solution in PEG400.

by a frequent amplification of the JAK2 locus and high levels of constitutive JAK2/STAT signaling. Inhibitor **29** was evaluated in HDLM-2[21] (cHL) tumor xenografts in SCID/NOD mouse. As shown in Figure 5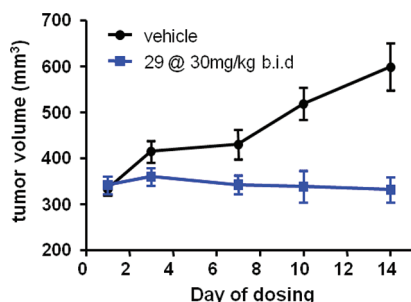A, compound **29** exhibited dose related tumor growth inhibition with oral dosing at 30 mg/kg bid for 19 days and 55 mg/kg bid for 7 days; the 55 mg/kg group was switched to a single daily dose schedule (qd) at day 7 due to moderate body weight loss (<10% average). Despite switching to qd dosing with the 55 mg/kg group, a dose-related response was maintained in the efficacy study up to day 19. The increase of tumor volume in the treated groups beginning around day 12 was likely due to a clonal selection of more resistant cells in the tumors in response to treatment. A dose related increase in plasma (7 and 9 μM, respectively) and tumor levels (6 and 10 μM, respectively) were observed at 3 h post last dose, Figure 5B.

CONCLUSION

Optimization of the 1,2,4-triazolo[1,5-*a*]pyridine scaffold as a kinase hinge binding element led to the discovery of a novel, selective JAK2 inhibitor. The optimization process was greatly enhanced by the straightforward synthetic sequence developed. The readily prepared, multisubstituted 1,2,4-triazolo[1,5-*a*]-pyridine core was sequentially appended via Suzuki−Miyaura cross coupling followed by a Buchwald−Hartwig coupling to provide desired targets.

The developed SAR led to the understanding that *para* substitution of the aryl ring at the C8-position of the core was optimal, with the methanesulfonyl moiety displaying excellent JAK2 potency. The serendipitous discovery of enhanced JAK2 selectivity based solely on moving a saturated heterocycle from

the *para* to the *meta* position on the solvent exposed side of the molecule was key to reducing the potential risk of immune suppression related to undesired JAK3 inhibition. The *N*-methylpiperazine heterocycle resulted in excellent intrinsic and cellular potency. The moderate basicity of the heterocycle enhanced the physiochemical properties of this scaffold to achieve oral bioavailability. CEP-33779,[22] **29**, exhibited excellent JAK2 potency, selectivity, and oral bioavailability in mouse. Additionally, **29** has demonstrated antitumor efficacy in multiple JAK2-driven tumor xenografts and efficacy in inflammation models in mouse and has potential as a preclinical development candidate.

EXPERIMENTAL SECTION

General Methods. All commercial reagents and solvents were used as received unless otherwise indicated. ^{1}H and ^{13}C NMR spectra were recorded on a Bruker Avance spectrometer at 400 or 100 MHz, respectively, in the deuterated solvent noted with tetramethylsilane as the internal standard. Mass spectrometry (LC/MS) data were collected on either an Agilent 1100 series HPLC coupled to Bruker Esquire 2000 ion trap mass spectrometer (2.1 mm × 30 mm Agilent Eclipse XBD C8 3.5 μm column, elution with 10−100% acetonitrile and water with 0.1% formic acid solvent gradient, over 5 min) or a Waters Acquity Ultra Performance LC coupled to a Waters Micromass ZQ quadropole mass spectrometer (2.1 mm × 30 mm Acquity BEH C18 1.7 μm column, elution with 5−95% acetonitrile and water with 0.1% formic acid solvent gradient, over 2 min) and are reported as (M + H)+, i.e., molecular ion plus hydrogen. Analytical HPLC data was collected using an Agilent 1100 series HPLC coupled with an Agilent Eclipse XDB C18 5 μm (4.6 mm × 150 mm) column, elution with 10−100% acetonitrile and water (with 0.1% trifluoroacetic acid as modifier) solvent gradient, over 5 min. Reverse phase chromatography was performed with a Gilson apparatus coupled to a Phenomenex Gemini-NX C18 5 μm column, either (150 mm × 30 mm) or (100 mm × 21 mm) using an acetonitrile and water (with 0.1% trifluoroacetic acid as modifier) solvent gradient. Automated normal phase chromatography was performed with a Teledyne ISCO CombiFlash Companion apparatus using RediSep Rf flash columns (SiO$_2$ or amine modified SiO$_2$). Melting point temperatures were collected using a Mel-Temp device and are uncorrected. Compounds have ≥95% purity except where indicated and compound purity is listed as the area percentage (A%) [peak mAU·s/total mAU·s] at a wavelength of 254 nm.

Select Examples. *Phenyl-[1,2,4]triazolo[1,5-a]pyridin-2-yl-amine (9, X and R = H).* To a suspension of 1-phenyl-3-pyridin-2-yl-thiourea (1.00 g, 4.40 mmol) in acetonitrile (6 mL) was added dimethyl sulfate (0.45 mL, 4.8 mmol) and heated at reflux for 4 h, cooled to room temperature, and the volatiles were evaporated to yield
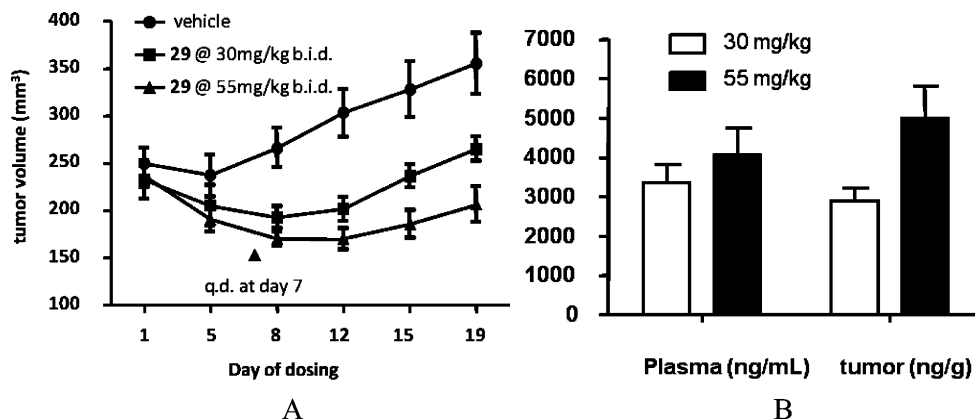

Figure 5. Results of PK and efficacy experiment in HDLM-2 xenograft in SCID/NOD mouse: (A) antitumor efficacy of **29**, dosed po as a solution in PEG400, 55 mg/kg bid switched to qd dosing at day 7, (B) plasma and tumor compound levels at 3 h post last dose.

viscous yellow oil. To a solution of the yellow oil in dichloromethane (8 mL) was added hydroxylamine hydrochloride (0.67 g, 9.6 mmol) followed by *N,N*-diisopropylethylamine (3.3 mL, 19.0 mmol). The mixture was stirred at room temperature for 18 h. Water (10 mL) was added, and a nitrogen sparge tube connected to a bleach scrubber was fitted to the reaction flask. The mixture was sparged with nitrogen. The resulting oily liquid was partitioned between ethyl acetate (100 mL) and water (20 mL). The organic layer was washed with water (3 × 20 mL), dried over magnesium sulfate, filtered, and evaporated to a waxy solid. To a cooled solution of waxy solid in acetonitrile (10 mL) at −5 °C was added potassium carbonate (1.5 g, 0.011 mol) followed by dropwise addition of 20% phosgene in toluene (2.6 mL, 4.9 mmol). The mixture was stirred for 1 h at −5 °C and then warmed to room temperature. Additional 20% phosgene in toluene (1.0 mL) and potassium carbonate (1.0 g) was added to the mixture and stirred for 48 h. The volatiles were evaporated, and the residue was partitioned between ethyl acetate (100 mL) and water (20 mL). The organic layer was washed with water (3 × 20 mL), dried over magnesium sulfate, filtered, and evaporated to an orange waxy solid. The product (0.17 g, 18% yield) was isolated via column chromatography (silica gel 40 g, 5%→100% ethyl acetate/heptane). ^{1}H NMR (CDCl$_3$) δ 8.46−8.42 (m, 1H), 7.63−7.59 (m, 2H), 7.51−7.41 (m, 2H), 7.38−7.33 (m, 2H), 7.31 (br s, 1H), 7.02−6.97 (m, 1H), 6.90−6.85 (m, 1H). ^{13}C NMR (CDCl$_3$) δ 162.51, 150.24, 140.38, 129.60, 129.16, 127.85, 121.37, 117.19, 113.83, 111.96; mp 180−184 °C. High resolution mass spectrum (ESI+) *m/z* 211.0990 [(M + H)$^+$ calcd for C$_{12}$H$_{10}$N$_4$: 211.0984]. HPLC: 96 A%.

8-(2-Methoxy-phenyl)-[1,2,4]triazolo[1,5-a]pyridin-2-ylamine (12). To a solution of 3-bromo-pyridin-2-ylamine (10.0 g, 57.8 mmol) in 1,4-dioxane (100 mL) was added dropwise ethoxycarbonyl isothiocyanate (6.8 mL, 58 mmol). The mixture was stirred under nitrogen for 18 h and then volatiles were evaporated. The recovered material was triturated with hexane (250 mL) and then filtered. The off-white solid was added to a stirred suspension of hydroxylamine hydrochloride (20.0 g, 288 mmol) and *N,N*-diisopropylethylamine (30.0 mL, 172 mmol) in a mixture of methanol (80 mL) and ethanol (80 mL). A nitrogen sparge tube connected to a bleach scrubber was fitted to the reaction flask. The mixture was stirred at room temperature for 2 h, heated to 60 °C for 18 h, and then cooled to room temperature. The suspension was filtered, rinsed with methanol and then water and methanol again. 8-Bromo-[1,2,4]triazolo[1,5-a]pyridin-2-ylamine (11) was isolated as an off-white solid (9.66 g, 78%). ^{1}H NMR (DMSO-*d*$_6$) δ 8.58 (d, *J* = 6.5 Hz, 1H), 7.73 (d, *J* = 7.5 Hz, 1H), 6.80 (dd, *J* = 7.0, 7.0 Hz, 1H), 6.25 (br s, 2H); mp 219−222 °C. LC/MS (ESI+) *m/z* 213.05, 214.80 (M + H)$^+$. HPLC: 85 A%

A dry tube was charged with palladium acetate (0.10 g, 0.47 mmol), triphenylphosphine (0.31 g, 1.2 mmol), and 1,4-dioxane (5 mL) and then purged under vacuum then backflushed and stirred under nitrogen for 10 min. 8-Bromo-[1,2,4]triazolo[1,5-a]pyridin-2-ylamine (11) (0.50 g, 2.3 mmol), 2-methoxybenzeneboronic acid (0.71 g, 4.7 mmol), *N,N*-dimethylformamide (5 mL), and 1.50 M of sodium carbonate in water (4.7 mL, 7.0 mmol) were added, respectively. The tube was sealed, and the reaction mixture was heated at 80 °C for 18 h. The mixture was cooled to room temperature and transferred to a round-bottom flask, and the volatiles were evaporated under reduced pressure. 8-(2-Methoxy-phenyl)-[1,2,4]triazolo[1,5-a]pyridin-2-ylamine (12) (0.41 g, 34%) was isolated via column chromatography (amine modified silica gel 47 g, 0%→10% methanol/dichloromethane). ^{1}H NMR (DMSO-*d*$_6$) δ 8.50 (dd, *J* = 6.6,1.0 Hz, 1H), 7.51 (dd, *J* = 7.5,1.6 Hz, 1H), 7.43−7.36 (m, 2H), 7.13 (d, *J* = 8.2 Hz, 1H), 7.03 (t, *J* = 7.3 Hz, 1H), 6.91 (t, *J* = 6.8 Hz, 1H), 5.97 (br s, 2H), 3.73 (s, 3H). ^{13}C NMR (DMSO-*d*$_6$) δ 165.92, 156.57, 149.81, 131.10, 129.46, 129.01, 126.29, 124.65, 122.73, 120.02, 111.53, 110.78, 55.47; mp 200−202 °C. LC/MS (ESI+) *m/z* 240.98 (M + H)$^+$. HPLC: 97 A%.

8-Pyridin-3-yl-[1,2,4]triazolo[1,5-a]pyridin-2-ylamine (13). ^{1}H NMR (DMSO-*d*$_6$) δ 9.28 (d, *J* = 2.1 Hz, 1H), 8.62−8.58 (m, 2H), 8.49 (m, 1H), 7.82 (dd, *J* = 7.4, 0.7 Hz, 1H), 7.53 (dd, *J* = 8.0, 4.7 Hz, 1H), 7.01 (t, *J* = 7.0 Hz, 1H), 6.18 (br s, 2H). ^{13}C NMR (DMSO-*d*$_6$) δ

166.17, 148.91, 148.84, 135.40, 131.17, 127.31, 126.90, 123.32, 121.18, 111.46; mp 185−187 °C. LC/MS (ESI+) *m/z* 211.99 (M + H)$^+$. HPLC: 91 A%.

8-Pyridin-4-yl-[1,2,4]triazolo[1,5-a]pyridin-2-ylamine (14). ^{1}H NMR (DMSO-*d*$_6$) δ 8.69 (dd, *J* = 4.8, 1.4 Hz, 2H), 8.65 (dd, *J* = 6.5, 0.8 Hz, 1H), 8.18 (dd, *J* = 4.7, 1.6 Hz, 2H), 7.94 (dd, *J* = 7.5, 0.9 Hz, 1H), 7.03 (t, *J* = 6.8 Hz, 1H), 6.24 (s, 2H). ^{13}C NMR (DMSO-*d*$_6$) δ 166.23, 149.82, 148.85, 142.48, 128.16, 127.44, 122.27, 120.94, 111.34; mp 209−215 °C. LC/MS (ESI+) *m/z* 212.00 (M + H)$^+$. HPLC: 92 A%.

8-(6-Methoxy-pyridin-3-yl)-[1,2,4]triazolo[1,5-a]pyridin-2-ylamine (15). ^{1}H NMR (DMSO-*d*$_6$) δ 8.91 (d, *J* = 2.5 Hz, 1H), 8.54 (dd, *J* = 6.6, 0.9 Hz, 1H), 8.44 (dd, *J* = 8.7, 2.5 Hz, 1H), 7.73 (dd, *J* = 7.6, 1.0 Hz, 1H), 6.97 (t, *J* = 6.9 Hz, 1H), 6.96 (d, *J* = 8.7 Hz, 1H), 6.12 (s, 2H), 3.92 (s, 3H). ^{13}C NMR (DMSO-*d*$_6$) δ 166.01, 163.15, 148.81, 146.32, 138.69, 126.54, 125.74, 124.74, 121.29, 111.46, 109.96, 53.28; mp 157−158 °C. LC/MS (ESI+) *m/z* 241.95 (M + H)$^+$. HPLC: 89 A%.

8-(3-Methanesulfonyl-phenyl)-[1,2,4]triazolo[1,5-a]pyridin-2-ylamine (16). ^{1}H NMR (DMSO-*d*$_6$) δ 8.64−8.60 (m, 1H), 8.59 (t, *J* = 1.6 Hz, 1H), 8.50−8.46 (m, 1H), 7.98−7.94 (m, 1H), 7.86−7.83 (m, 1H), 7.78 (dd, *J* = 7.8, 7.8 Hz, 1H), 7.02 (dd, *J* = 7.1, 7.1 Hz, 1H), 6.18 (s, 1H), 3.29 (S, 3H). ^{13}C NMR (DMSO-*d*$_6$) δ 166.17, 148.91, 141.17, 136.59, 133.11, 129.51, 127.49, 127.36, 126.30, 126.21, 122.39, 111.44, 43.48; mp 173−183 °C. LC/MS (ESI+) *m/z* 289.03 (M + H)$^+$. HPLC: 85 A%.

8-(4-Methanesulfonyl-phenyl)-[1,2,4]triazolo[1,5-a]pyridin-2-ylamine Hydrochloride (17). ^{1}H NMR (DMSO-*d*$_6$) δ 8.69−8.65 (m, 1H), 8.37−8.32 (m, 2H), 8.07−8.02 (m, 2H), 7.88−7.85 (m, 1H), 7.11−7.06 (m, 1H), 5.32 (br s, 3H), 3.29 (s, 3H). ^{13}C NMR (DMSO-*d*$_6$) δ 165.40, 148.23, 140.14, 140.03, 128.95, 128.21, 127.90, 127.03, 122.31, 111.98, 43.51; mp 237−239 °C. High resolution mass spectrum (ESI+) *m/z* 289.0767 [(M + H)$^+$ calcd for C$_{13}$H$_{12}$N$_4$O$_2$S: 289.0759]. HPLC: 98 A%.

8-(4-Trifluoromethyl-phenyl)-[1,2,4]triazolo[1,5-a]pyridin-2-ylamine (18). ^{1}H NMR (DMSO-*d*$_6$) δ 8.62 (d, *J* = 6.3 Hz, 1H), 8.34 (d, *J* = 8.0 Hz, 2H), 7.88−7.80 (m, 3H), 7.02 (t, *J* = 6.8 Hz, 1H), 6.18 (s, 2H); mp 186−187 °C. LC/MS (ESI+) *m/z* 279.05 (M + H)$^+$. HPLC: 91 A%.

[8-(2-Methoxy-phenyl)-[1,2,4]triazolo[1,5-a]pyridin-2-yl]-phenyl-amine (19). ^{1}H NMR (CDCl$_3$) δ 8.42 (dd, *J* = 6.6, 0.9 Hz, 1H), 7.62 (dd, *J* = 7.5, 1.7, 1H), 7.58−7.52 (m, 3H), 7.44−7.38 (m, 1H), 7.36−7.30 (m, 2H), 7.10 (t, *J* = 7.5 Hz, 1H), 7.05 (d, *J* = 8.3 Hz, 1H), 6.97 (t, *J* = 7.4 Hz, 1H), 6.93 (t, *J* = 7.1 Hz, 1H), 6.87 (s, 1H), 3.82 (s, 3H); mp 141−145 °C. LC/MS (ESI+) *m/z* 317.06 (M + H)$^+$. HPLC: 89 A%.

[8-(3-Methanesulfonyl-phenyl)-[1,2,4]triazolo[1,5-a]pyridin-2-yl]-phenyl-amine (20). ^{1}H NMR (CDCl$_3$) δ 8.68 (t, *J* = 1.8 Hz, 1H), 8.49 (dd, *J* = 6.7, 1.3 Hz, 1H), 8.38 (m, 1H), 8.01 (m, 1H), 7.74 (dd, *J* = 7.8, 7.8 Hz, 1H), 7.70−7.60 (m, 5H), 7.58−7.51 (m, 1H), 7.49−7.43 (m, 2H), 7.40−7.34 (m, 2H), 7.04−6.99 (m, 2H), 6.91 (s, 1H), 3.14 (s, 3H); mp 184−191 °C. LC/MS (ESI+) *m/z* 365.04 (M + H)$^+$. HPLC: 82 A%.

[8-(4-Methanesulfonyl-phenyl)-[1,2,4]triazolo[1,5-a]pyridin-2-yl]-phenyl-amine (21). ^{1}H NMR (CDCl$_3$) δ 8.51 (dd, *J* = 6.6, 0.9 Hz, 1H), 8.26−8.21 (m, 2H), 8.11−8.06 (m, 2H), 7.66 (dd, *J* = 7.3, 0.9 Hz, 1H), 7.61−7.57 (m, 2H), 7.39−7.32 (m, 2H), 7.05−6.99 (m, 2H), 6.94 (s, 1H), 3.10 (s, 3H); mp 197−201 °C. LC/MS (ESI+) *m/z* 365.11 (M + H)$^+$. HPLC: 79 A%.

[8-(4-Methanesulfonyl-phenyl)-[1,2,4]triazolo[1,5-a]pyridin-2-yl]-(2-methoxy-phenyl)-amine (22). ^{1}H NMR (CDCl$_3$) δ 8.53−8.49 (m, 1H), 8.38 (dd, *J* = 8.0, 1.3 Hz, 1H), 8.24 (d, *J* = 8.4 Hz, 2H), 8.10 (d, *J* = 8.5 Hz, 2H), 7.66−7.62 (m, 1H), 7.61 (s, 1H), 7.08−6.89 (m, 4H), 3.92 (s, 3H), 3.11 (s, 3H); mp 211−213 °C. LC/MS (ESI+) *m/z* 395.10 (M + H)$^+$. HPLC: 88 A%.

[8-(4-Methanesulfonyl-phenyl)-[1,2,4]triazolo[1,5-a]pyridin-2-yl]-(3-methoxy-phenyl)-amine (23). ^{1}H NMR (CDCl$_3$) δ 8.50 (d, *J* = 6.1 Hz, 1H), 8.24 (d, *J* = 7.8 Hz, 2H), 8.08 (d, *J* = 7.7 Hz, 2H), 7.66 (d, *J* = 7.4 Hz, 1H), 7.37 (s, 1H), 7.28−7.22 (m, 1H), 7.08−7.00 (m, 2H), 6.92 (s, 1H), 6.58 (d, *J* = 7.6 Hz, 1H), 3.86 (s, 3H), 3.10 (s, 3H); mp 204−206 °C. LC/MS (ESI+) *m/z* 395.15 (M + H)$^+$. HPLC: 90 A%.

*[8-(4-Methanesulfonyl-phenyl)-[1,2,4]triazolo[1,5-a]pyridin-2-yl]-(4-methoxy-phenyl)-amine (**24**).* ^{1}H NMR (CDCl$_3$) δ 8.47 (d, J = 6.6 Hz, 1H), 8.23 (d, J = 8.5 Hz, 2H), 8.09 (d, J = 8.5 Hz, 2H), 7.64 (d, J = 7.4 Hz, 1H), 7.00 (dd, J = 6.8, 6.8 Hz, 1H), 6.95–6.90 (m, 2H), 6.71 (s, 1H), 3.82 (s, 3H), 3.10 (s, 3H); mp 208–212 °C. LC/MS (ESI+) m/z 395.13 (M + H)$^+$. HPLC: 89 A%.

*(3-Methanesulfonyl-phenyl)-[8-(4-methanesulfonyl-phenyl)-[1,2,4]triazolo[1,5-a]pyridin-2-yl]-amine (**25**).* ^{1}H NMR (CDCl$_3$) δ 8.55 (d, J = 6.9 Hz, 1H), 8.47 (s, 1H), 8.26 (d, J = 7.9 Hz, 2H), 8.12 (d, J = 7.5 Hz, 2H), 7.74–7.69 (m, 2H), 7.58–7.50 (m, 2H), 7.17 (s, 1H), 7.12–7.07 (m, 1H), 3.11 (s, 6H); mp 230–234 °C. LC/MS (ESI+) m/z 443.11 (M + H)$^+$. HPLC: 94 A%.

*(4-Methanesulfonyl-phenyl)-[8-(4-methanesulfonyl-phenyl)-[1,2,4]triazolo[1,5-a]pyridin-2-yl]-amine (**26**).* ^{1}H NMR (CDCl$_3$) δ 8.56 (d, J = 5.7 Hz, 1H), 8.22 (d, J = 8.0 Hz, 2H), 8.10 (d, J = 7.6 Hz, 2H), 7.92 (d, J = 7.8 Hz, 2H), 7.77 (d, J = 7.3 Hz, 2H), 7.72 (d, J = 7.3 Hz, 1H), 7.32 (s, 1H), 7.14–7.09 (m, 1H), 3.11 (s, 3H), 3.06 (s, 3H); mp 280–282 °C. LC/MS (ESI+) m/z 443.10 (M + H)$^+$. HPLC: 92 A%.

*[8-(4-Methanesulfonyl-phenyl)-[1,2,4]triazolo[1,5-a]pyridin-2-yl]-(3-morpholin-4-yl-phenyl)-amine (**27**).* ^{1}H NMR (CDCl$_3$) δ 8.50 (dd, J = 6.6, 1.1 Hz, 1H), 8.26–8.22 (m, 2H), 8.10–8.05 (m, 2H), 7.66 (dd, J = 7.3, 1.1 Hz, 1H), 7.36 (t, J = 2.2 Hz, 1H), 7.25 (t, J = 8.0 Hz, 1H), 7.05–6.98 (m, 2H), 6.85 (s, 1H), 6.59 (dd, J = 8.3, 1.9 Hz, 1H), 3.91–3.87 (m, 4H), 3.24–3.20 (m, 4H), 3.10 (s, 3H); mp 234–236 °C. LC/MS (ESI+) m/z 450.17 (M + H)$^+$. HPLC: 94 A%.

*[8-(4-Methanesulfonyl-phenyl)-[1,2,4]triazolo[1,5-a]pyridin-2-yl]-(4-morpholin-4-yl-phenyl)-amine (**28**).* To an oven-dried tube was added 8-(4-methanesulfonyl-phenyl)-[1,2,4]triazolo[1,5-a]pyridin-2-ylamine (100.0 mg, 0.3468 mmol), 4-(4-bromo-phenyl)-morpholine (100.0 mg, 0.4130 mmol), palladium acetate (10.0 mg, 0.0445 mmol), and 9,9-dimethyl-4,5-bis(diphenylphosphino)xanthene (75.0 mg, 0.130 mmol), cesium carbonate (240.0 mg, 0.7366 mmol), and 1,4-dioxane (5 mL). The mixture was purged under vacuum and backflushed with nitrogen three times. The tube was sealed and heated at 80 °C for 72 h. The mixture was cooled to room temperature and diluted with dichloromethane (10 mL), filtered, and the filtrate was evaporated. The product (0.063 g, 40%) was isolated via column chromatography (silica gel 40 g, 20%→100% ethyl acetate/hexane). ^{1}H NMR (CDCl$_3$) δ 8.49–8.45 (m, 1H), 8.25–8.20 (m, 2H), 8.11–8.06 (m, 2H), 7.63 (dd, J = 7.4, 0.9 Hz, 1H), 7.53–7.48 (m, 2H), 6.99 (t, J = 7.0 Hz, 1H), 6.97–6.93 (m, 2H), 6.73 (s, 1H), 3.90–3.86 (m 4H), 3.14–3.09 (m, 7H); mp 244–246 °C. LC/MS (ESI+) m/z 450.08 (M + H)$^+$. HPLC: 88 A%.

*[8-(4-Methanesulfonyl-phenyl)-[1,2,4]triazolo[1,5-a]pyridin-2-yl]-[3-(4-methyl-piperazin-1-yl)-phenyl]-amine (**29**).* To an oven-dried tube was added 8-(4-methanesulfonyl-phenyl)-[1,2,4]triazolo[1,5-a]pyridin-2-ylamine (50.0 mg, 0.173 mmol), 1-(3-bromo-phenyl)-4-methyl-piperazine (53.0 mg, 0.208 mmol), palladium acetate (8.0 mg, 0.036 mmol), 2,2′-bis-dicyclohexylphosphanyl-biphenyl (20.0 mg, 0.0366 mmol), cesium carbonate (140.0 mg, 0.4297 mmol), and 1,4-dioxane (2 mL) under an atmosphere of nitrogen. The tube was vacuum purged and backflushed with nitrogen three times and then the tube was sealed and the mixture was heated at 100 °C for 3 days. The reaction mixture was cooled to room temperature diluted with dichloromethane (10 mL), filtered, and the filtrate was evaporated. The product was isolated (0.029 g, 36%) via column chromatography (amine modified silica gel 47 g, 0%→10% methanol:dichloromethane). ^{1}H NMR (CDCl$_3$) δ 8.49 (dd, J = 6.6, 1.0 Hz, 1H), 8.25 (d, J = 8.4 Hz, 2H), 8.08 (d, J = 8.4 Hz, 2H), 7.66 (dd, J = 7.5, 0.9 Hz, 1H), 7.39–7.36 (m, 1H), 7.23 (t, J = 8.2 Hz, 1H), 7.02 (t, J = 7.1 Hz, 1H), 6.97 (dd, J = 7.8, 1.4 Hz, 1H), 6.88 (s, 1H), 6.60 (dd, J = 8.3, 1.8 Hz, 1H), 3.30–3.25 (m, 4H), 3.10 (s, 3H), 2.63–2.58 (m, 4H), 2.38 (s, 3H). ^{13}C NMR (CDCl$_3$) δ 162.65, 152.28, 148.87, 141.00, 140.91, 140.05, 129.64, 129.29, 128.18, 127.85, 127.76, 124.77, 112.03, 109.40, 108.59, 104.80, 55.19, 49.02, 46.19, 44.59; mp 208–211 °C. High resolution mass spectrum (ESI+) m/z 463.1925 [(M + H)$^+$ calcd for C$_{24}$H$_{26}$N$_6$O$_2$S: 463.1916]. HPLC: 95 A%.

*[8-(4-Methanesulfonyl-phenyl)-[1,2,4]triazolo[1,5-a]pyridin-2-yl]-[4-(4-methyl-piperazin-1-yl)-phenyl]-amine (**30**).* ^{1}H NMR (CDCl$_3$)

δ 8.47 (dd, J = 6.7, 1.1 Hz, 1H), 8.25–8.20 (m, 2H), 8.10–8.06 (m, 2H), 7.63 (dd, J = 7.4, 1.1 Hz, 1H), 7.51–7.46 (m, 2H), 7.01–6.95 (m, 2H), 6.67 (s, 1H), 3.20–3.15 (m, 4H), 3.10 (s, 3H), 2.62–2.58 (m, 4H), 2.36 (s, 3H); mp 242–244 °C. LC/MS (ESI+) m/z 463.13 (M + H)$^+$. HPLC: 91 A%.

*[8-(4-Methanesulfonyl-phenyl)-[1,2,4]triazolo[1,5-a]pyridin-2-yl]-[3-(4-methyl-piperazin-1-ylmethyl)-phenyl]-amine (**31**).* ^{1}H NMR (CDCl$_3$) δ 8.51 (d, J = 6.6 Hz, 1H), 8.24 (d, J = 8.5 Hz, 2H), 8.09 (d, J = 8.5 Hz, 2H), 7.66 (dd, J = 7.4, 0.9 Hz, 1H), 7.58 (dd, J = 7.8, 1.9 Hz, 1H), 7.46 (s, 1H), 7.31 (t, J = 7.8 Hz, 1H), 7.02 (t, J = 7.2 Hz, 1H), 6.98 (d, J = 7.5 Hz, 1H), 6.90 (s, 1H), 3.54 (s, 2H), 3.10 (s, 3H), 2.70–2.32 (m, 8H), 2.29 (s, 3H). LC/MS (ESI+) m/z 477.18 (M + H)$^+$. HPLC: 90 A%.

*N-{3-[(1,1-Dioxidothiomorpholin-4-yl)methyl]phenyl}-8-[4-(methylsulfonyl)phenyl][1,2,4]triazolo[1,5-a]pyridin-2-amine (**32**).* ^{1}H NMR (CDCl$_3$) δ 8.52 (dd, J = 6.7, 1.0 Hz, 1H), 8.23 (d, J = 8.H Hz, 2H), 8.09 (d, J = 8.4 Hz, 2H), 7.68 (dd, J = 7.4, 0.9 Hz, 1H), 7.62–7.60 (m, 1H), 7.48 (dd, J = 8.1, 1.8 Hz, 1H), 7.32 (t, J = 7.7 Hz, 1H), 7.05 (t, J = 7.1 Hz, 1H), 6.97–6.93 (m, 2H), 3.70 (s, 2H), 3.13–3.01 (m, 11H). LC/MS (ESI+) m/z 512.08 (M + H)$^+$. HPLC: 94 A%.

*[8-(4-Methanesulfonyl-phenyl)-[1,2,4]triazolo[1,5-a]pyridin-2-yl]-[3-(4-morpholin-4-yl-piperidin-1-yl)-phenyl]-amine (**33**).* ^{1}H NMR (CDCl$_3$) δ 8.49 (d, J = 6.4 Hz, 1H), 8.26 (d, J = 8.0 Hz, 2H), 8.08 (d, J = 7.1 Hz, 2H), 7.66 (d, J = 8.0 Hz, 1H), 7.35 (s, 1H), 7.24–7.18 (m, 1H), 7.01 (d, J = 6.7 Hz, 1H), 6.96 (d, J = 7.9 Hz, 1H), 6.84 (s, 1H), 6.60 (d, J = 8.4 Hz, 1H), 3.81 (d, J = 11.7 Hz, 2H), 3.77–3.72 (m, 4H), 3.10 (s, 3H), 2.78 (t, J = 11.8 Hz, 2H), 2.63–2.58 (m, 4H), 2.40–2.30 (m, 1H), 1.97 (d, J = 12.7 Hz, 2H), 1.74–1.62 (m, 2H); mp 230–236 °C. LC/MS (ESI+) m/z 533.16 (M + H)$^+$. HPLC: 94 A%.

*[8-(4-Methanesulfonyl-phenyl)-[1,2,4]triazolo[1,5-a]pyridin-2-yl]-{3-[4-(4-methyl-piperazin-1-yl)-piperidin-1-yl]-phenyl}-amine (**34**).* ^{1}H NMR (CDCl$_3$) δ 8.49 (d, J = 6.5 Hz, 1H), 8.25 (d, J = 6.9 Hz, 2H), 8.08 (d, J = 7.7 Hz, 2H), 7.65 (d, J = 7.1 Hz, 1H), 7.31 (s, 1H), 7.24–7.18 (m, 1H), 7.04–6.95 (m, 2H), 6.82 (s, 1H), 6.60 (d, J = 7.9 Hz, 1H), 3.81 (d, J = 11.4 Hz, 2H), 3.10 (s, 3H), 2.77 (t, J = 12.2 Hz, 2H), 2.72–2.33 (m, 9H), 2.30 (s, 3H), 1.96 (d, J = 11.2 Hz, 2H), 1.75–1.63 (m, 2H); mp 237–239 °C. LC/MS (ESI+) m/z 546.20 (M + H)$^+$. HPLC: 94 A%.

*[8-(4-Methanesulfonyl-phenyl)-[1,2,4]triazolo[1,5-a]pyridin-2-yl]-[3-(1-methyl-piperidin-4-yl)-phenyl]-amine (**35**).* ^{1}H NMR (CDCl$_3$) δ 8.51 (d, J = 6.5 Hz, 1H), 8.08 (d, J = 8.3 Hz, 2H), 8.10 (d, J = 7.3 Hz, 2H), 7.66 (d, J = 6.6 Hz, 1H), 7.55 (s, 1H), 7.38 (d, J = 8.7 Hz, 1H), 7.31–7.25 (m, 1H), 7.02 (t, J = 7.4 Hz, 1H), 6.91–6.85 (m, 2H), 3.10 (s, 3H), 3.01 (d, J = 10.9 Hz, 2H), 2.57–2.45 (m, 1H), 2.35 (S, 3H), 2.11–2.03 (m, 2H), 1.92–1.83 (m, 4H); mp 208–210 °C. LC/MS (ESI+) m/z 462.16 (M + H)$^+$. HPLC: 91 A%.

*[3-(4-Methyl-piperazin-1-yl)-phenyl]-{8-[4-(propane-2-sulfonyl)-phenyl]-[1,2,4]triazolo[1,5-a]pyridin-2-yl}-amine (**36**).* ^{1}H NMR (CDCl$_3$) δ 8.49 (d, J = 6.7 Hz, 1H), 8.27 (d, J = 7.7 Hz, 2H), 8.01 (d, J = 7.9 Hz, 2H), 7.67 (d, J = 7.3 Hz, 1H), 7.39 (s, 1H), 7.26–7.20 (m, 1H), 7.04–6.95 (m, 2H), 6.85 (s, 1H), 6.60 (d, J = 7.7 Hz, 1H), 3.31–3.19 (m, 5H), 2.63–2.58 (m, 4H), 2.38 (s, 3H), 1.35 (d, J = 6.7 Hz, 6H). LC/MS (ESI+) m/z 491.19 (M + H)$^+$. HPLC: 85 A%.

*[3-(4-Methyl-piperazin-1-yl)-phenyl]-[8-(4-trifluoromethyl-phenyl)-[1,2,4]triazolo[1,5-a]pyridin-2-yl]-amine (**37**).* ^{1}H NMR (CDCl$_3$) δ 8.46 (d, J = 7.0 Hz, 1H), 8.15 (d, J = 7.7 Hz, 2H), 7.76 (d, J = 8.2 Hz, 2H), 7.62 (d, J = 7.2 Hz, 1H), 7.48 (s, 1H), 7.25–7.19 (m, 1H), 7.02–6.97 (m, 2H), 6.92 (d, J = 7.3 Hz, 1H), 6.83 (s, 1H), 6.59 (d, J = 7.8 Hz, 1H), 3.30–3.25 (m, 4H), 2.62–2.57 (m, 4H), 2.37 (s, 3H); mp 234–236 °C. LC/MS (ESI+) m/z 453.15 (M + H)$^+$. HPLC: 97 A%.

*[8-(4-Fluoro-phenyl)-[1,2,4]triazolo[1,5-a]pyridin-2-yl]-[3-(4-methyl-piperazin-1-yl)-phenyl]-amine (**38**).* ^{1}H NMR (DMSO-d_6) δ 9.56 (s, 1H), 8.78 (d, 1H), 8.20 (m, 2H), 7.85 (d, 1H), 7.50 (s, 1H), 7.35 (m, 2H), 7.10 (m, 3H), 6.45 (m, 1H), 3.12 (m, 4H), 2.46 (m, 4H), 2.23 (s, 3H); mp 194–196 °C. LC/MS (ESI+) m/z 403 (M + H)$^+$. HPLC: 95 A%.

*{8-[4-(Dimethyl-phosphinoyl)-phenyl]-[1,2,4]triazolo[1,5-a]pyridin-2-yl]-[3-(4-methyl-piperazin-1-yl)-phenyl]-amine (**39**).* ^{1}H NMR (CDCl$_3$) δ 8.46 (d, J = 6.2 Hz, 1H), 8.15 (d, J = 8.0 Hz, 2H), 7.92–7.84 (m, 2H), 7.63–7.50 (m, 1H), 7.34 (s, 1H), 7.23 (t, J =

8.2 Hz, 1H), 7.02–6.96 (m, 2H), 6.84 (s, 1H), 6.59 (d, J = 7.8 Hz, 1H), 3.30–3.25 (m, 4H), 2.63–2.58 (m, 4H), 2.37 (s, 3H), 1.80 (s, 3H), 1.77 (s, 3H); mp 243–246 °C. LC/MS (ESI+) m/z 461.0 (M + H)$^+$. HPLC: 100 A%.

[8-(4-Methanesulfonyl-phenyl)-6-trifluoromethyl-[1,2,4]triazolo-[1,5-a]pyridin-2-yl]-[4-(4-methyl-piperazin-1-yl)-phenyl]-amine (40). ^{1}H NMR (CDCl$_3$) δ 8.82 (s, 1H), 8.25 (d, J = 7.8 Hz, 2H), 8.13 (d, J = 7.3 Hz, 2H), 7.79 (s, 1H), 7.49 (d, J = 8.2 Hz, 2H), 6.99 (d, J = 8.2 Hz, 2H), 6.88 (s, 1H), 3.21 (bm, 4H), 3.13 (s, 3H), 2.66 (bm, 4H), 2.40 (s, 3H); mp 126–134 °C. LC/MS (ESI+) m/z 531.0 (M + H)$^+$. HPLC: 98 A%.

[6-Fluoro-8-(4-methanesulfonyl-phenyl)-[1,2,4]triazolo[1,5-a]-pyridin-2-yl]-[4-(4-methyl-piperazin-1-yl)-phenyl]-amine (41). ^{1}H NMR (CDCl$_3$) δ 8.45 (s, 1H), 8.26 (d, J = 8.0 Hz, 2H), 8.11 (d, J = 7.7 Hz, 2H), 7.58 (d, J = 9.0 Hz, 1H), 7.48 (dd, J = 11.5 Hz, 7.8 Hz, 2H), 6.98 (d, J = 7.9 Hz, 2H), 6.76 (s, 1H), 3.27 (bm, 4H), 3.12 (s, 3H), 2.62 (bm, 4H), 2.38 (s, 3H); mp 130–138 °C. LC/MS (ESI+) m/z 481.2 (M + H)$^+$. HPLC: 95 A%.

Enzyme Assays for JAK1, JAK2, and JAK3. The kinase activity of baculovirus-expressed human JAK1, JAK2, or JAK3 was measured using the time-resolved fluorescence detection system as previously described.[23] Each 96-well Costar high binding plate (Corning, Corning, NY) was coated with 100 µL/well of 10 µg/mL neutravidin (Pierce Biotechnology, Rockford, IL) in TBS at 37 °C for 2 h, followed by 100 µL/well of 1 µg/mL 15-mer peptide substrate (biotinyl-amino-hexanoyl-EQEDEPEGDYFEWLE-amide, Infinity Bio-tech Research and Resource, Aston, PA) at 37 °C for 1 h. The kinase assay mixture (total volume = 100 µL/well) consisting of 20 mM HEPES (pH 7.2), ATP (0.2 µM ATP for JAK1 and JAK2 and 0.1 µM ATP for JAK3), 1 mM MnCl$_2$, 0.1% BSA, and test compound (diluted in DMSO, 2.5% DMSO final in assay) was added to the assay plate. Enzyme was added and the reaction was allowed to proceed for 20 min at room temperature (RT). Detection of the phosphorylated product was performed by adding 100 µL/well of diluted Eu–N1 labeled PY100 antibody (PerkinElmer, Boston, MA). Samples were incubated at RT for 1 h, followed by addition of 100 µL enhancement solution (PerkinElmer). Plates were agitated for 10 min, and the fluorescence of the resulting solution measured using the PerkinElmer EnVision 2102 or 2104 multilabel plate reader. IC$_{50}$ values were determined using the 4-parameter logistic model in XLFit 4 (IDBS, Ltd., Guildford, UK).

Cell-Based Assay for JAK2. The JAK2 cell-based assay was performed using a modified GeneBLAzer assay for the CellSensor irf1-bla TF-1 cell line.[23] Cryopreserved cells were suspended at 1.25×10^6 cells/mL in assay media containing modified DMEM/F12 (Invitrogen, Carlsbad, CA), 0.5% dialyzed FBS, 2 mM glutamine (Invitrogen), 100 U/mL penicillin, and 100 µg/mL streptomycin (Mediatech, Manassas, VA). The cell suspension (40 µL/well) was dispensed into the 384-well assay plates (Corning, Corning, NY) and incubated overnight at 5% CO$_2$, 37 °C. Test compound/DMSO (100 nL) was then added to the assay plates. For the negative control wells, an internal JAK2 reference inhibitor was delivered at a concentration that produced 100% inhibition; positive control wells received only DMSO. Assay plates were incubated for 1 h prior to adding 5 µL/well of GM-CSF (Invitrogen) diluted in assay media (1 ng/mL final concentration in assay, equivalent to its EC$_{80}$). The plates were then incubated for 5 h at 5% CO$_2$, 37 °C. Development was initiated by addition of 8 µL LiveBLAzer FRET β-lactamase loading solution per well (Invitrogen), and the plate was incubated for 4 h at RT. Detection was performed on the EnVision 2102 plate reader (PerkinElmer). IC$_{50}$ values were determined using the 4-parameter logistic model in XLFit 4 (IDBS, Ltd.).

PK Assay. Adult animals (Charles River, Kingston, New York; n = 3/time point) were used in all experiments. IV administration was via the lateral tail vein, and oral doses were administered by gavage using a fixed dose volume of 100 µL. Compounds were administered IV in a vehicle of 25% hydroxyl-propyl-β-cyclodextrin and formulated in 100% PEG400 for oral dosing. The mice were sacrificed by decapitation, and trunk blood was collected into heparinized tubes at predetermined sampling times through 6 or 24 h. The blood samples were placed on

wet ice until centrifuged to separate plasma. The plasma fraction was transferred into clean, dry tubes, frozen on dry ice, and stored at approximately −20 °C pending analysis. Plasma samples were analyzed for test compounds using a preliminary method, consisting of high-performance liquid chromatography (HPLC) coupled with tandem mass spectrometry. Pharmacokinetic parameters were estimated using noncompartmental methods.

PD Assay. Nude mice bearing CWR22 xenografts were dosed orally with 55 mg/kg of compound **29** or a vehicle (PEG400). At 2, 6, and 24 h after dosing animals (3/group) were sacrificed, tumors were excised and plasma samples were prepared. Tumor extracts were prepared using Triton-based extraction buffer supplemented with inhibitors of proteases and phosphatases. Equal amounts of extracts were resolved on SDS-PAGE gels and STAT3 phosphorylation and expression were analyzed by Western blot using specific antibodies (Cell Signaling). Specific bands were quantified using the GelPro program and STAT3 activation in each sample was determined as a ratio of phosphoSTAT3/total STAT3. Results were graphed as a mean STAT3 phophorylation per group relative to the vehicle group which was set at 100%.

Efficacy Studies. CWR22 prostate carcinoma cells or HDLM-2 (classical Hodgkin lymphoma) cells were injected into the flanks of nude (CWR22) or SCID/NOD mice. After tumors became palpable, animals were grouped (10 mice/group) and dosed with a vehicle (PEG400) or 30 mg/kg bid (CWR22) or 30 mg/kg bid and 55 mg/kg bid (HDLM-2) of compound **29**. Tumor volume was measured every 3–4 days.

■ ASSOCIATED CONTENT

Accession Codes

Atomic coordinates for the cocrystal structure of JAK2 with inhibitor **28** can be accessed using PDB code 4AQC.

■ AUTHOR INFORMATION

Corresponding Author

*Phone: 610-738-6733. Fax: 610-738-6643. E-Mail: bdugan@cephalon.com.

Notes

The authors declare no competing financial interest.

■ ACKNOWLEDGMENTS

■ ABBREVIATIONS USED

JAK, Janus kinase; STAT, signal transduction and transcription; TYK, tyrosine kinase; TPP, triphenylphosphine; SCID/NOD, severe combined immune deficiency/nonobese diabetic; MQL, minimum quantifiable level

■ REFERENCES

(1) (a) Yu, H.; Jove, R. The STATs of Cancer—New Molecular Targets Come of Age. *Nature Rev. Cancer* **2004**, *4*, 97−105. (b) Dagvadorj, A.; Collins, S.; Jomain, J.-B.; Abdulghani, J.; Karras, J.; Zellweger, T.; Li, H.; Nurmi, M.; Alanen, K.; Mirtti, T.; Visakorpi, T.; Bubendorf, L.; Goffin, V.; Nevalainen, M. T. Autocrine Prolactin Promotes Prostate Cancer Cell Growth via Janus Kinase-2-Signal Transducer and Activator of Transcription-5a/b Signaling Pathway. *Endocrinology* **2007**, *148*, 3089−3101. (c) Pardanani, A. JAK2 Inhibitor Therapy in Myeloproliferative Disorders: Rationale, Preclinical Studies and Ongoing Clinical Trials. *Leukemia* **2008**, *22*, 22−30.

(2) (a) Kortylewski, M.; Kujawski, M.; Wang, T.; Wei, S.; Zhang, S.; Pilon-Thomas, S.; Niu, G.; Kay, H.; Mule, J.; Kerr, W. G.; Jove, R.; Pardoll, D.; Yu, H. Inhibiting Stat3 Signaling in the Hematopoietic System Elicits Multicomponent Antitumor Immunity. *Nature Med.* **2005**, *11*, 1314−1321. (b) Nefedova, Y.; Gabrilovich, D. I. Targeting of Jak/STAT Pathway in Antigen Presenting Cells in Cancer. *Curr. Cancer Drug Targets* **2007**, *7*, 71−77.

(3) (a) Lin, W.-W.; Karin, M. A cytokine-mediated link between innate immunity, inflammation, and cancer. *J. Clin. Invest.* **2007**, *117*, 1175−1183. (b) Pardanani, A. JAK2 inhibitor therapy in myeloproliferative disorders: rationale, preclinical studies and ongoing clinical trials. *Leukemia* **2008**, *22*, 23−30. (c) Marotta, L. L. C.; Almendro, V.; Marusyk, A.; Shipitsin, M.; Schemme, J.; Walker, S. R.; Bloustain-Qimron, N.; Kim, J. J.; Choudhury, S. A.; Maruyama, R.; Wu, Z.; Gönen, M.; Mulvey, L. A.; Bessarabova, M. O.; Huh, S. J.; Silver, S. J.; Kim, S. Y.; Park, S. Y.; Lee, H. E.; Anderson, K. S.; Richardson, A. L.; Nikolskaya, T.; Nikolsky, Y.; Liu, X. S.; Root, D. E.; Hahn, W. C.; Frank, D. A.; Polyak, K. The JAK2/STAT3 signaling pathway is required for growth of CD44+CD24− stem cell-like breast cancer cells in human tumors. *J. Clin. Invest.* **2011**, *121*, 2723−2735.

(4) Manning, G.; Whyte, D. B.; Martinez, R.; Hunter, T.; Sundarsanam, S. The Protein Kinase Complement of the Human Genome. *Science* **2002**, *298*, 1912.

(5) (a) Li, H.; Ahonen, T. J.; Alanen, K.; Xie, J.; LeBaron, M. J.; Pretlow, T. G.; Ealley, E. L.; Zhang, Y.; Nurmi, M.; Singh, B.; Martikainen, P. M.; Nevalainen, M. T. Activation of Signal Transducer and Activator of Transcription 5 in Human Prostate Cancer is Associated with High Histological Grade. *Cancer Res.* **2004**, *64*, 4774−4782. (b) Tan, S.-H.; Nevalainen, M. T. Signal Transducer and Activator of Transcription 5A/B in Prostate and Breast Cancers. *Endocr.-Relat. Cancer* **2008**, *15*, 367−390. (c) Quintas-Cardama, A.; Kantarjian, H.; Cortes, J.; Verstovsek, S. Janus Kinase Inhibitors for the Treatment of Myeloproliferative Neoplasias and Beyond. *Nature Rev. Drug Discovery* **2011**, *10*, 127−140.

(6) (a) Borie, D. C.; Si, M.-S.; Morris, R. E.; Reitz, B. A.; Changelian, P. S. JAK3 inhibition as a new concept for immune suppression. *Curr. Opin. Invest. Drugs* **2003**, *4*, 1297−1303. (b) O'Shea, J. J.; Pesu, M.; Borie, D. C.; Changelian, P. S. A New Modality for Immunosuppression: Targeting the JAK/STAT Pathway. *Nature Rev. Drug Discovery* **2004**, *4*, 555−564.

(7) (a) Flex, E.; Petrangeli, V.; Stella, L.; Chiaretti, S.; Hornakova, T.; Knoops, L.; Ariola, C.; Fodale, V.; Clappier, E.; Paoloni, F.; Martinelli, S.; Fragale, A.; Sanchez, M.; Tavolaro, S.; Messina, M.; Cazzaniga, G.; Camera, A.; Pizzolo, G.; Tornesello, A.; Vignetti, M.; Battistini, A.; Cave, H.; Gelb, B. D.; Renauld, J.-C.; Biondi, A.; Constantinescu, S. N.; Foa, R.; Tartaglia, M. Somatically acquired *JAK1* mutations in adult acute lymphoblastic leukemia. *J. Exp. Med.* **2008**, *205*, 751−758. (b) Minegishi, Y.; Saito, M.; Morio, T; Watanabe, K.; Agematsu, K.; Tsuchiya, S.; Takada, H.; Hara, T.; Kawamura, N.; Ariga, T.; Kaneko, H.; Konda, N.; Tsuge, I.; Yachie, A.; Sakiyama, Y.; Iwata, T.; Bessho, F.; Ohishi, T.; Joh, K.; Imai, K.; Kogawa, K.; Shinohara, M.; Fujieda, M.; Wakiguchi, H.; Pasic, S.; Abinun, M.; Ochs, H. D.; Renner, E. D.; Jansson, A.; Belohradsky, B. H.; Metin, A.; Shimizu, N.; Mizutani, S.; Miyawaki, T.; Nonoyama, S.; Karasuyama, H. Human Tyrosine Kinase 2 Deficiency Reveals Its Requisite Roles in Multiple Cytokine Signals Involved in Innate and Acquired Immunity. *Immunity* **2006**, *25*, 745−755.

(8) Tyner, J. W.; Bumm, T. G.; Deininger, J.; Wood, L.; Aichberger, K. J.; Loriaux, M. M.; Druker, B. J.; Burns, C. J.; Fantino, E.; Deininger, M. W. CYT387, a novel JAK2 inhibitor, induces hematologic responses and normalizes inflammatory cytokines in murine myeloproliferative neoplasms. *Blood* **2010**, *115*, 5232−5240.

(9) Pardanani, A.; Gotlib, J. R.; Jamieson, C.; Cortes, J. E.; Talpaz, M.; Stone, R. M.; Silverman, M. H.; Gilliland, D. G.; Schorr, J.; Tefferi, A. Safety and Efficacy of TG101348, a Selective JAK2 Inhibitor, in Myelofibrosis. *J. Clin. Oncol.* **2011**, *29*, 789−796.

(10) (a) Shilling, A. D.; Nedza, F. M.; Emm, T.; Diamond, S.; McKeever, E.; Punwani, N.; Williams, W.; Arvanitis, A.; Galya, L. G.; Li, M.; Shepard, S.; Rodgers, J.; Yue, T.-Y.; Yeleswaram, S. Metabolism, Excretion, and Pharmacokinetics of [^{14}C]INCB018424, a Selective Janus Tyrosine Kinase 1/2 Inhibitor, in Humans. *Drug Metab. Dispos.* **2010**, *38*, 2023−2031. (b) Ruxolitinib was granted approval by the United States Food and Drug administration on November 16, 2011: http://www.fda.gov/NewsEvents/Newsroom/PressAnnouncements/ucm280102.htm.

(11) Hevdat, M.; Huszar, D.; Herrmann, A.; Gozgit, J. M.; Schroeder, A.; Sheehy, A.; Buettner, R.; Proia, D.; Kowolik, C. M.; Xin, H.; Armstrong, B.; Bebernitz, G.; Weng, S.; Wang, L.; Ye, M.; McEachern, K.; Chen, H.; Morosini, D.; Bell, K.; Alimzhanov, M.; Ioannidis, S.; McCoon, P.; Cao, Z. A.; Yu, H.; Jove, R.; Zinda, M. The JAK2 Inhibitor AZD1480 Potently Blocks Stat3 Signaling and Oncogenesis in Solid Tumors. *Cancer Cell* **2009**, *16*, 487−497.

(12) Hexner, E. O.; Serdikoff, C.; Jan, M.; Swider, C. R.; Robinson, C.; Yang, S.; Angeles, T.; Emerson, S. G.; Carroll, M.; Ruggeri, B.; Dobrzanski, P. Lestaurtinib (CEP701) is a JAK2 inhibitor that suppresses JAK2/STAT5 signaling and the proliferation of primary erythroid cells from patients with myeloproliferative disorders. *Blood* **2008**, *111*, 5663−5671.

(13) William, A. D.; Lee, A. C.-H.; Blanchard, S.; Poulsen, A.; Teo, E. L.; Nagaraj, H.; Tan E. Chen, D.; Williams, M.; Sun, E. T.; Goh, K. C.; Ong, W. C.; Goh, S. K.; Hart, S.; Jayaraman, R.; Pasha, M. K.; Ethirajulu, K.; Wood, J. M.; Dymock, B. W. Discovery of the Macrocycle 11-(2-Pyrrolidin-1-yl-ethoxy)-14,19-dioxa-5,7,26-triaza-tetracyclo[19.3.1.1(2,6).1(8,12)]heptacosa-1(25),2(26),3,5,8,10,12(27),16,21,23-decaene (SB1518), a Potent Janus 2/Fms-like Tyrosine Kinase-3 (JAK2/FLT3) Inhibitor for the Treatment of Myelofibrosis and Lymphoma. *J. Med. Chem.* **2011**, *54*, 4638−4658.

(14) Nettekoven, M.; Püllmann, B.; Schmitt, S. Synthetic Access to 2-Amido-5-aryl-8-methoxy-triazolopyridine and 2-Amido-5-morpholino-8-methoxy-triazolopyridine Derivatives as Potential Inhibitors of the Adenosine Receptor Subtypes. *Synthesis* **2003**, 1649−1652.

(15) (a) Zificsak, C. A.; Gingrich, D. E.; Breslin, H. J.; Dunn, D. D; Milkiewicz, K. L.; Theroff, J. P.; Thieu, T. V.; Underiner, T. L.; Weinberg, L. R.; Aimone, L. D.; Albom, M. S.; Mason, J. L.; Saville, L.; Husten, J.; Angeles, T. S.; Finn, J. P.; Jan, M.; O'Kane, T. M.; Dobrzanski, P.; Dorsey, B. D. Optimization of a novel kinase inhibitor scaffold for the dual inhibition of JAK2 and FAK kinases. *Bioorg. Med. Chem. Lett.* **2012**, *22*, 133−137. (b) Weinberg, L. R.; Albom, M. S.; Angeles, T. S.; Breslin, H. J.; Gingrich, D. E.; Huang, Z.; Lisko, J. G.; Mason, J. L.; Milkiewicz, K. L.; Thieu, T. T.; Underiner, T. L.; Wells, G. J.; Wells-Knect, K. J.; Dorsey, B. D. 2,7-Pyrrolo[2,1-*f*][1,2,4]-triazines as JAK2 inhibitors: modification of target structure to minimize reactive metabolite formation. *Bioorg. Med. Chem. Lett.* **2011**, *21*, 7325−7330.

(16) (a) Potts, K. T.; Burton, H. R.; Bhattacharyya, J. Derivatives of *s*-Triazolo[1,5-*a*]pyridine Ring System. *J. Org. Chem.* **1966**, *31*, 260−265. (b) Potts, K. T.; Burton, H. R.; Roy, S. K. Reactions of the *s*-Triazolo[4,3-*a*]pyridine Ring System. *J. Org. Chem.* **1966**, *31*, 265−273. (c) Potts, K. T.; Surapaneni, C. R. 1,2,4-Triazoles. XXV. The Effect of Pyridine Substitution on the Isomerization of *s*-Triazolo[4,3-*a*]pyridines into *s*-Triazolo[1,5-*a*]pyridines. *J. Heterocycl. Chem.* **1970**, *7*, 1019−1027. (d) Verček, B.; Ogorevc, B.; Stanovnik, B.; Tišler, M. Cyanoamino Compounds in Synthesis: Syntheses of Some Heterocycles. *Monatsch. Chem.* **1983**, *114*, 789−798.

(17) Bell, B. M.; Fanwick, P. E.; Graupner, P. R.; Roth, G. A. Application of the Tisler Triazolopyrimidine Cyclization to the Synthesis of a Crop Protection Agent and an Intermediate. *Org. Process Res. Dev.* **2006**, *10*, 1167−1171.

(18) Swinnen, D.; Jorand-Lebrun, C.; Grippi-Vallotton, T.; Muzerelle, M.; Royle, A.; Macritchie, J; Hill, R.; Shaw, J. P. Preparation of triazolopyridines as apoptosis signal-regulating kinase (ASK) inhibitors for treatment of autoimmune, inflammatory, cardiovascular, and/or neurodegenerative diseases. Patent WO2009/027283A1, 2009.

(19) (a) Wang, Y.; Shakespeare, W. C.; Huang, W.-S.; Sundaramoorthi, R.; Lentini, S.; Das, S.; Liu, S.; Banda, G.; Wen, D.; Zhu, X.; Xu, Q.; Keats, J.; Wang, F.; Wardwell, S.; Ning, Y.; Snodgrass, J. T.; Broudy, M. I.; Russian, K.; Dalgarno, D.; Clackson,

T.; Sawyer, T. K. Novel N[9]-arenethenyl purines as potent dual Src/Abl tyrosine kinase inhibitors. *Bioorg. Med. Chem. Lett.* **2008**, *18*, 4907–4912. (b) Shakespeare, W. C.; Metcalf, C. A.; Sawyer, T. K.; Wang, Y.; Sundaramoorthi, R.; Dalgarno, D. C.; Bohacek, R.; Weigele, M. Substituted Purine Derivatives. Patent WO2005/009348A2, 2005.

(20) (a) Kinase selectivity was determined using the Ambit Bioscience KINOMEscan technology, and is expressed as S(90), the fraction of kinases inhibited ≥90% when screened at 1 μM across a panel of 402 kinases. (b) Karaman, M. W.; Herrgard, S.; Treiber, D. K.; Gallant, P.; Atteridge, C. E.; Campbell, B. T.; Chan, K. W.; Ciceri, P.; Davis, M. I.; Edeen, P. T.; Faraoni, R.; Floyd, M.; Hunt, J. P.; Lockhart, D. J.; Milanov, Z. V.; Morrison, M. J.; Pallares, G.; Patel, H. K.; Pritchard, S.; Wodicka, L. M.; Zarrinkar, P. P. A Quantitative Analysis of Kinase Inhibitor Selectivity. *Nature Biotechnol.* **2008**, *26*, 127.

(21) Cochet, O.; Frelin, C.; Peyron, J.-F.; Imbert, V. Constitutive activation of STAT proteins in the HDLM-2 and L540 Hodgkin lymphoma-derived cell lines supports cell survival. *Cell. Signalling* **2006**, *18*, 449–455.

(22) (a) Stump, K. L.; Lu, L. D.; Dobrzanski, P.; Serdikoff, C.; Gingrich, D. E.; Dugan, B. J.; Angeles, T. S.; Albom, M. S.; Ator, M. A.; Dorsey, B. D.; Ruggeri, B. A.; Seavey, M. M. A highly selective, orally active inhibitor of Janus kinase 2, CEP-33779, ablates disease in two mouse models of rheumatoid arthritis. *Arthritis Res. Ther.*. **2011**, *13*, R68. (b) Seavey, M. M.; Lu, L. D.; Stump, K. L.; Wallace, N. H; Hockeimer, W.; O'Kane, T. M.; Ruggeri, B.; Dobrzanski, P. Therapeutic Efficacy of CEP-33779, a Novel Selective JAK2 Inhibitor, in a Mouse Model of Colitis-induced Colorectal Cancer. *Mol. Cancer Ther.* **2012**, *11*, 984–993.

(23) Mason, J., L.; Holskin, B. P.; Murray, K. A.; Meyer, S. L.; Ator, M. A.; Angeles, T. S. Modification of CellSensor Irf1-bla TF-1 and Irf1-bla HEL Assays for Direct Comparison of Wild-type JAK2 and JAK2 V617F Inhibition. *Assay Drug Dev. Technol.* **2011**, *9*, 311–318.